

Development of a Polymersome Blood Ammonia Assay Coupled with a Portable Near-Infrared Fluorometer

Published as part of ACS Bio & Med Chem Au virtual special issue “2024 Rising Stars in Biological, Medicinal, and Pharmaceutical Chemistry”.

Marie-Lynn Al-Hawat, Justine Caron, Sarah Djebbar, and Simon Matoori*



Cite This: ACS Bio Med Chem Au 2024, 4, 226–232



Read Online

ACCESS |



Metrics & More



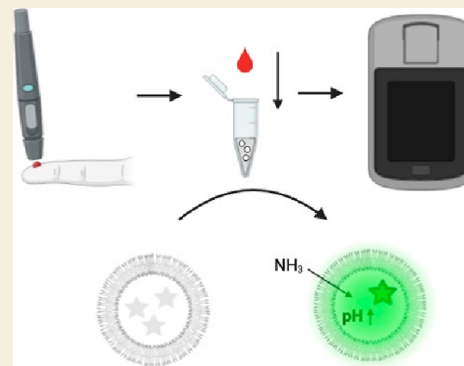
Article Recommendations



Supporting Information

ABSTRACT: Ammonia is a key biomarker in inborn and acquired liver disease. As clinical point-of-care blood ammonia assays are lacking, we developed a polymersome formulation for point-of-care blood ammonia sensing combined with a portable fluorometer. A pH-sensitive near-infrared (NIR) fluorescent dye was identified, which showed a strong fluorescence increase at acidic pH values. Building on reports on ammonia-selective PS-*b*-PEG polymersomes, these polymersomes were loaded with the NIR dye. These NIR fluorescent polymersomes sensed ammonia in a clinically relevant range in ammonia-spiked fresh whole blood with high linearity ($R^2 = 0.9948$) after 5 min using a conventional tabletop plate reader. Subsequently, the assay was tested with a portable fluorometer. An ammonia-dependent fluorescence increase was detected in ammonia-spiked fresh mouse blood after 5 min using the portable fluorometer. The NIR dye-loaded PS-*b*-PEG polymersomes rapidly sensed ammonia with high linearity in whole blood. This assay was successfully combined with a portable fluorometer and only required 3 μL of blood. These findings motivate a further development and clinical translation of this point-of-care blood ammonia assay.

KEYWORDS: fluorometer, ammonia, ammonia assay, polymersome, point-of-care, diagnostics



1. INTRODUCTION

Ammonia is an endogenous metabolite with important roles in pH homeostasis and protein metabolism.¹ However, at pathologically elevated blood concentrations (hyperammonemia), ammonia exerts neurotoxic effects.² The liver is the principal organ that removes ammonia in the body. Patients with inborn (e.g., urea cycle disorders, UCD) or acquired liver disease (e.g., liver cirrhosis and acute liver failure) often fall short of efficiently clearing ammonia.¹ Ammonia subsequently accumulates in the brain and results in neuropsychiatric symptoms (cognitive impairments, somnolence, hepatic coma, and in some cases, death).³ This syndrome termed hepatic encephalopathy (HE) occurs in 30–40% of patients with liver cirrhosis.⁴ The plasma ammonia cutoff is 50 μM for adults and 100 μM for newborns^{5,6} and can reach values up to 400 μM .⁷ The clinical gold standard for plasma ammonia testing (glutamate dehydrogenase assay) has a lower limit of quantification of 17 μM according to the manufacturer's information (AM1015, Randox Laboratories).

Despite the important role of ammonia in liver disease, there are currently no Food and Drug Administration-cleared point-of-care tests for ammonia. The clinical gold standard is a glutamate dehydrogenase-based absorbance test in plasma that requires analysis in the hospital laboratory and thus is not

suitable for point-of-care or bedside testing.⁸ Point-of-care ammonia testing is a clinical care gap as it would allow for rapid ammonia determination at the bedside for acute hyperammonemic crises and surveillance of chronic HE and UCD patients in the outpatient setting. Such a point-of-care ammonia assay would complement the clinical evaluation of patients with liver disease, accelerating clinical decision-making and allowing for ammonia monitoring at home.

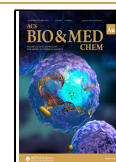
Transmembrane pH-gradient polymersomes have recently gained interest for their ammonia detoxification and sensing capacity.^{9–11} High-glass-transition-temperature polymersomes made of poly(styrene)-*b*-poly(ethylene glycol) (PS-*b*-PEG) are highly suited for sequestration of ammonia due to their higher ammonia selectivity and stability than transmembrane pH-gradient liposomes.^{12–14} When these polymersomes are exposed to ammonia, ammonia diffuses into the acidic polymersome core and increases the luminal pH (Figure

Received: March 7, 2024

Revised: June 23, 2024

Accepted: July 16, 2024

Published: July 30, 2024



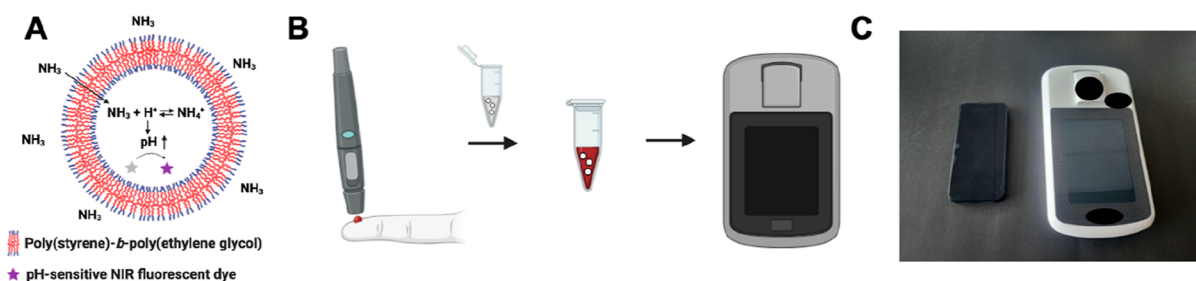


Figure 1. Polymersome ammonia assay and portable fluorometer. Mechanism of action of polymersome ammonia assay: ammonia diffuses across the membrane of transmembrane pH-gradient poly(styrene)-*b*-poly(ethylene glycol) polymersomes into the acidic core. The protonation of ammonia increases the luminal pH and the fluorescence intensity of an encapsulated pH-sensitive NIR fluorescent dye (A). In the proposed ammonia assay setup, capillary blood is collected by a fingerstick and added to a polymersome assay solution. The NIR fluorescence change is detected by a portable fluorometer (B). Portable fluorometer used in this study compared with an iPhone 13 as a size reference (C). NIR: near-infrared fluorescent.

1A). This pH increase can be quantified by a pH-sensitive fluorophore and can thus be used for ammonia sensing. PS-*b*-PEG polymersomes loaded with the pH-sensitive fluorescent dye pyranine were capable of sensing ammonia in various biological fluids, namely, in the plasma of hyperammonemic rats.⁹ However, pyranine is not suited for blood ammonia sensing due to interference by hemoglobin. Also, these studies were performed using a large tabletop fluorescence plate reader. To translate this assay to the point of care, fluorescent dyes with low interference by hemoglobin and hand-held portable fluorescence detection systems are needed.

NIRF assays have the potential to reach the point of care.^{15–21} Thanks to the low interference of hemoglobin with NIRF dyes, there is no need for blood separation which is challenging to perform at the point of care.²² To detect the fluorescence signal at the point of care, small portable fluorometers are required.^{23,24} The miniaturization of fluorometers entails technical challenges to achieve trade-offs between dimensions and performance (e.g., limit of detection, accuracy, and precision).²⁵ Recent technical advances have made portable NIRF fluorometers more widely available. Building on recent reports on ammonia-sensing PS-*b*-PEG polymersomes,^{9,10} the aims of this study were to develop a NIRF dye-loaded polymersome formulation, to test it in fresh whole blood, and to combine this polymersome ammonia assay with a commercial portable NIR fluorometer (Figure 1B,C).

2. MATERIALS AND METHODS

2.1. Materials

Diblock copolymer methoxy-poly(ethylene glycol) 2000-*b*-poly(styrene) 3000 (mPEG(2000)-*b*-PS(3000)) was purchased from Advanced Polymer Materials (Dorval, Canada). Sodium chloride, sodium hydroxide, potassium phosphate monobasic, citric acid, sodium citrate, dimethyl sulfoxide (DMSO), trimethylamine, glycine, valine, levofloxacin, propranolol, and dichloromethane were purchased from Sigma-Aldrich (St. Louis, MO). IRDye 680RD NHS Ester was obtained from LI-COR Biosciences (Lincoln, USA). Purification columns (PD MidiTrap G-25 Columns) were obtained from Cytiva (Marlborough, USA).

2.2. Methods

2.2.1. Polymersome Preparation. The dye-containing polymersomes were prepared in accordance with the literature.⁹ 100 μ L of dichloromethane was used to dissolve 20 mg of mPEG(2000)-*b*-PS(3000) polymers. A solution of 1 mL of an isotonic citric acid solution 2.5 mM at pH 2.0 containing a concentration of IRDye 680RD was added to a 10 mL PFA vial (AHF Analysentechnik,

Tübingen, Germany) on ice. The polymer solution was added dropwise to the dye-containing citric acid solution under sonication with a probe sonotrode, Fisher Scientific model 705 Sonic Dismembrator, 700 W, 50/60 Hz, Fisher Scientific, Reinach, Switzerland) at an amplitude of 10 for 2 min in an ice bath. The organic solvent was evaporated for at least 10 min at 40 °C at 600 mbar using a rotary evaporator, except for the transmembrane pH gradient stability experiment, where evaporation was performed for 60 min at 40 °C at 220 mbar. The dispersion was stored at 4 °C and protected from light.

In accordance with the literature,⁹ MidiTrap G-25 columns were used to purify the fluorescent polymersomes to remove the free dye and replace the external phase with an isotonic sodium chloride-containing phosphate buffer 50 mM at pH 7.4. In brief, the columns were washed three times with the phosphate buffer. 200 μ L of the dye-containing polymersome dispersion and 800 μ L of the buffer solution were added. 750 μ L of the buffer was used to elute the purified polymersomes. They were then stored at 4 °C and protected from light.

The polymersome size was analyzed by laser diffraction (LS I3 320 Particle Size Analyzer, Beckman Coulter, Brea, CA) with isotonic 0.9% saline as the dispersion medium and presented as diameter (μ m) at the 10th (d10), 50th (median diameter, d50), and 90th percentile (d90) of the volume distribution.

2.2.2. pH Sensitivity of the Dye. An IRDye 680RD stock solution of 623 μ M was prepared in DMSO (Sigma-Aldrich). Citric acid solutions 50 mM were prepared at pH 1, 2, 3, 4, 5, and 6, and IRDye 680RD was diluted to a final concentration of 2 μ M. The fluorescence intensities of 100 μ L dye-containing solutions were read in a black 96-well plate by a plate reader (Tecan Spark Multimode Plate Reader, Tecan, Maennedorf, Switzerland) at the fluorescence excitation and emission wavelengths of 664 and 702 nm, respectively, with a bandwidth of 20 nm. This plate reader was equipped with a monochromator. The light intensity was not reported by the manufacturer. Device calibration with a fluorophore was not required according to the manufacturer. The fluorescence intensity of the same solutions (100 μ L) in 600 μ L Eppendorf tubes was also read by a portable fluorometer (Deniro, Detact Diagnostics, The Netherlands), whose emission and excitation wavelengths, bandwidth, and gain could not be changed. The specifications provided by the manufacturer include a processing time of <5 s per sample, an excitation LED source with a maximum at 760 nm, an emission filter at 750–769 nm, and detectors in the range of 800–1250 nm. The assay name “CoviTact” was used with a blank of phosphate buffer 50 mM at pH 7.4. The “Delta RFU” value was analyzed. The light intensity was not reported by the manufacturer. Device calibration with a fluorophore was not required according to the manufacturer. The stability of IRDye 680RD was tested by incubating the dye at 10 μ M in citric acid solution 50 mM at pH 2.0 a temperature of 4 °C for 5 days.

2.2.3. Blood Ammonia Sensing Using a Plate Reader. First, the polymersome assay was optimized in an isotonic sodium chloride-containing phosphate buffer at pH 7.4. The assay mixture was composed of 3 μL of mouse whole blood, 3 μL of ammonium chloride standard, purified polymersome dispersions at different volumes [25, 40, or 60 μL , resulting in polymersome dispersion volume percentages (v/v) of 25, 40, and 60%, respectively], and the volume was completed to 100 μL with isotonic phosphate buffer 50 mM at pH 7.4. The polymersome volume fraction represents the volume fraction of the purified polymersome dispersion in the total assay volume. A polymersome dispersion volume percentage of 60% was selected for the following experiments. To test the selectivity of the polymersomes toward ammonia in the presence of other amine-containing molecules, the polymersomes were incubated in an isotonic sodium chloride-containing phosphate buffer at pH 7.4 spiked with 100 μM ammonia in the presence of trimethylamine at 100 μM or a mix of molecules (glycine, valine, levofloxacin, and propranolol, each at 500 μM). To test its intra- and interday variability, the assay was performed with the same polymersome batches at 10 AM, at 4 PM of the same day, and in the following morning at 10 AM. The stability of the transmembrane pH gradient was investigated by fluorescence measurements of the dye-loaded polymersomes over the assay time of 30 min. Mouse blood was obtained from cardiac puncture with potassium EDTA as a coagulant in male C57BL6 mice (age 4 to 12 weeks) and immediately stored on ice. The blood samples were used within 40 min after collection. Ammonium chloride standards 0 to 0.5 mM were prepared in isotonic phosphate buffer 50 mM at pH 7.4. The assay mixture was composed of 3 μL of mouse whole blood, 3 μL of ammonium chloride standard, and 60 μL (60% v/v) of purified polymersome dispersion, and the volume was completed to 100 μL with isotonic phosphate buffer 50 mM at pH 7.4. The fluorescence intensity of a black 96 well plate was read after 2, 5, 10, 15, 20, 25, and 30 min using a plate reader at the fluorescence excitation and emission wavelengths described above. For the experiments in a blood-free medium, the blood volume was replaced with isotonic phosphate buffer (50 mM) at pH 7.4. The fluorescence ratio was defined as the fluorescence intensity at a given spiked ammonia concentration normalized to the fluorescence intensity of the nonspiked buffer or blood sample and allowed to compare different conditions. The lower limit of quantification was defined as the lowest spiked ammonia concentration with a coefficient of variation under 20%.

A limitation of this study is that the assay testing was performed in male mice at the age of 4 to 12 weeks. Future studies will investigate potential sex- and age-dependent effects on the assay performance in preclinical and clinical studies.

2.2.4. Blood Ammonia Sensing Using a Portable Fluorometer. The experiments were performed under point 2.2.3 with a polymersome volume of 90 μL (total volume of 100 μL). The assay mixture was prepared in a 600 μL Eppendorf tube. The fluorescence intensity of the tube was read after 2, 5, 10, 15, and 20 min and was determined by a portable fluorometer (Deniro, Detact Diagnostics, The Netherlands).

2.2.5. Statistical Analysis. GraphPad Prism (version 10.1.2) was used for the statistical analysis. Comparisons of three or more groups were performed by a one-way ANOVA followed by Tukey's posthoc test. Comparisons of the two groups were made using an unpaired *t*-test. A *p*-value of <0.05 was deemed statistically significant.

3. RESULTS AND DISCUSSION

3.1. pH-Dependent Fluorescence of IRDye 680RD

To determine the pH-dependent behavior of the NIR dye, the fluorescence intensity of IRDye 680RD was measured at different pH values. There was a pH-dependent increase in fluorescence intensity in the acidic range (Figure 2A,B). The pH-dependent increase was observed with both the tabletop and portable NIR fluorometer. We selected this dye hypothesizing that the protonation state of the nitrogen in

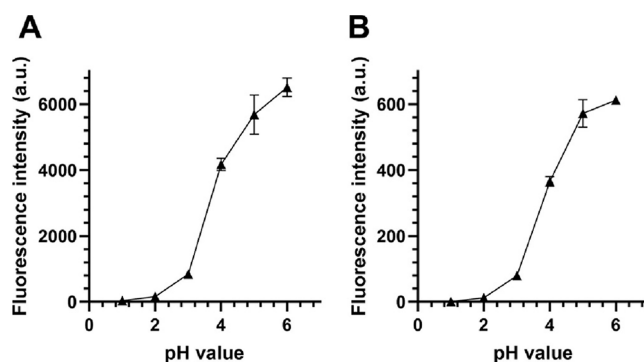


Figure 2. pH-dependent fluorescence of IRDye 680RD. Fluorescence intensity of IRDye 680RD at different pH values detected using a tabletop plate reader (A) and a portable fluorometer (B). IRDye 680RD concentration: 2 μM . All results are mean \pm SD ($n = 3$).

the indole ring affects the delocalization of the pi electrons and leads to a pH-dependent fluorescence intensity (Figure S1). Indeed, the deprotonation of the nitrogen at higher pH values increased the dye's fluorescence intensity. To study dye stability in an acidic buffer, the fluorescence intensity was investigated over 5 days, and no loss of fluorescence was observed (Figure S2).

3.2. Blood Ammonia Sensing Using a Plate Reader

To determine the usefulness of the NIR dye for the ammonia assay, it was encapsulated in PS-*b*-PEG polymersomes. In this section, the polymersomes were tested in buffer and fresh mouse blood and a tabletop plate reader was used as the detector. Fresh mouse blood is a suitable matrix as ammonia levels increase during storage.²⁶ In the buffer, there was an increase in the fluorescence intensity in a polymersome-concentration-dependent manner, which confirms that the polymersomes are the source of fluorescence (Figure 3A). The fluorescence intensity remained stable over 30 min. The polymersome volume fraction of 60% (v/v) was selected for the following experiments due to its high fluorescence intensity. Upon the addition of ammonia, there was an increase in the fluorescence intensity that reached a plateau after 15 min (Figure 3B). This gradual increase in fluorescence is likely due to the influx of ammonia into the polymersome core that increases the luminal pH and thus the fluorescence intensity of the dye. This finding is in line with the patent literature where an IRDye 680RD-loaded PS-*b*-PEG polymersome formulation was tested for ammonia sensing in phosphate buffer.²⁷ The increase in fluorescence was similar in whole blood (Figure 3B) which indicates that the ammonia sensing properties of the NIR dye-loaded polymersomes are preserved in whole blood and that the interference by hemoglobin is low.

In light of these encouraging findings with a single ammonia concentration, the IRDye 680RD-containing PS-*b*-PEG polymersomes were tested in a clinically relevant range of ammonia concentrations in HE and UCD of up to 500 μM .^{6,7,28–30} In ammonia-spiked whole blood, there was an ammonia concentration-dependent increase in fluorescence over time that reached a plateau after approximately 10 min (Figures 4A and S3). The response was highly linear ($R^2 = 0.9948$) in a clinically relevant ammonia range (Figure 4B). The whole blood volume fraction was 3 μL , a volume typically used in capillary blood assays.³¹ The lower limit of

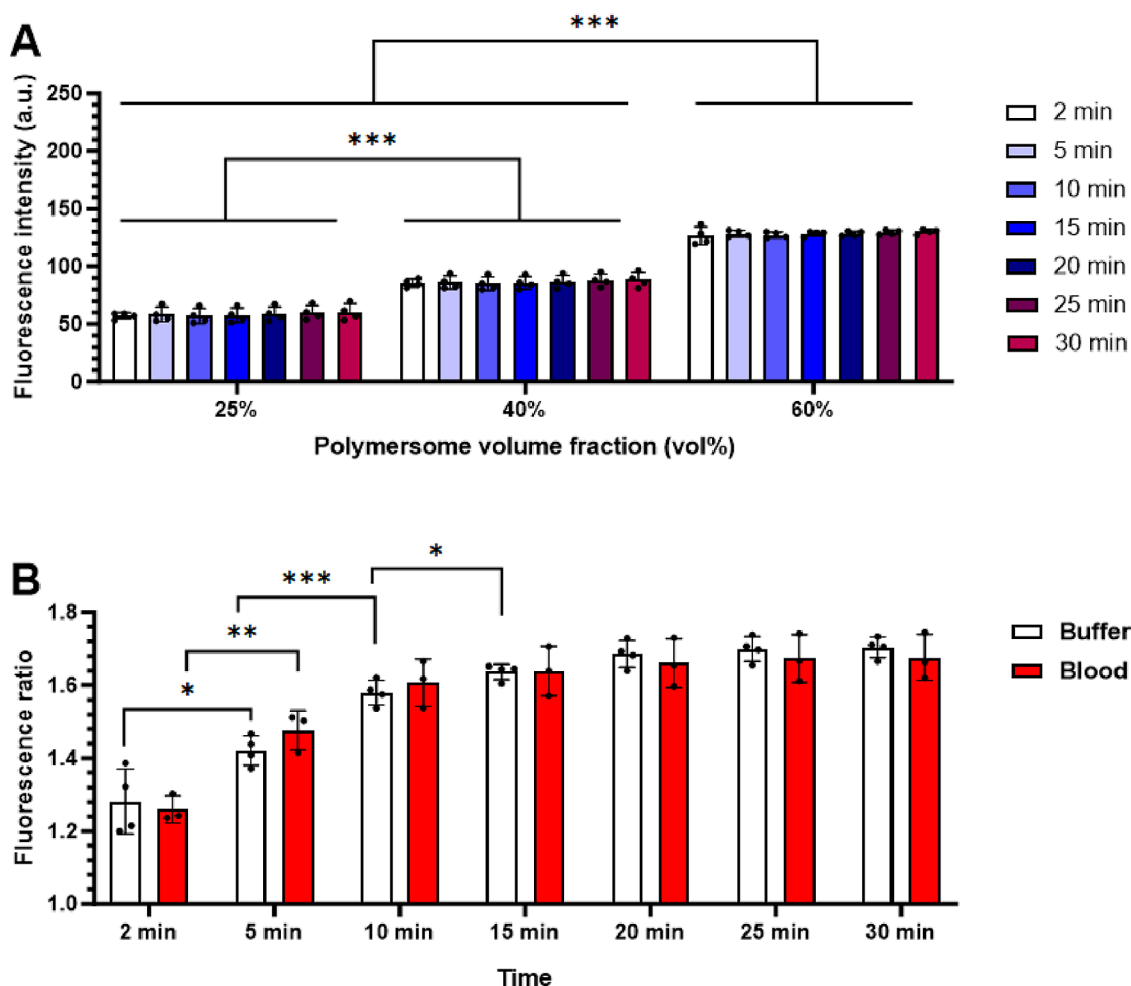


Figure 3. Ammonia sensing in ammonia-spiked buffer and mouse blood was carried out using a plate reader. Fluorescence intensity of IRDye 680RD-containing PS-*b*-PEG polymersomes at different volume fractions in ammonia-free isotonic phosphate buffer at pH 7.4 (A). Fluorescence intensity ratio of IRDye 680RD-containing PS-*b*-PEG polymersomes in ammonia-spiked buffer or blood over time (B). Fluorescence intensity ratio: fluorescence intensity in 0.5 mM ammonia-spiked buffer or blood normalized to nonspiked buffer or blood. Inner phase composition: dye concentration: 19 μM ; buffer composition of inner phase: isotonic citric acid buffer 2.5 mM at pH 2.0; whole blood volume fraction (B): 3% (v/v); incubation at room temperature. Detector: tabletop plate reader. All results are shown as means \pm SD ($n = 3-4$).

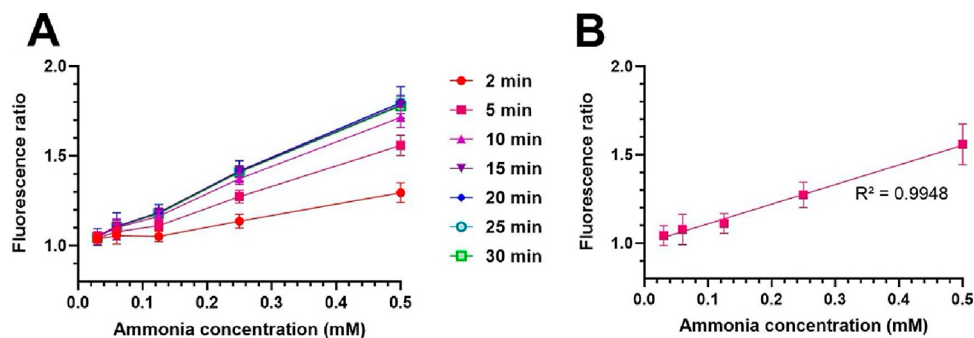


Figure 4. Ammonia sensing in ammonia-spiked mouse blood using a plate reader. Fluorescence intensity ratio of IRDye 680RD-containing PS-*b*-PEG polymersomes in ammonia-spiked blood over time (A). Fluorescence intensity ratio of IRDye 680RD-containing PS-*b*-PEG polymersomes in ammonia-spiked blood at 5 min with regression curve (B; data extracted from A). Fluorescence intensity ratio: fluorescence intensity of ammonia-spiked blood normalized to nonspiked blood. Inner phase composition: dye concentration: 37 μM ; buffer composition of inner phase: isotonic citric acid buffer 2.5 mM at pH 2.0; whole blood volume fraction: 3% (v/v); incubation at room temperature. Detector: tabletop plate reader. All results are means \pm SD ($n = 4$).

quantification was 31 μM after 2 min (coefficient of variation of 5.9%).

To test intra- and intraday variability of the assay, the response of the same polymersome batches was tested in an

ammonia-spiked buffer in the morning and afternoon and the following morning. A similar sensor response was observed at these time points (Figure S4). To study polymersome stability, the polymersome size was investigated over 5 days, and no

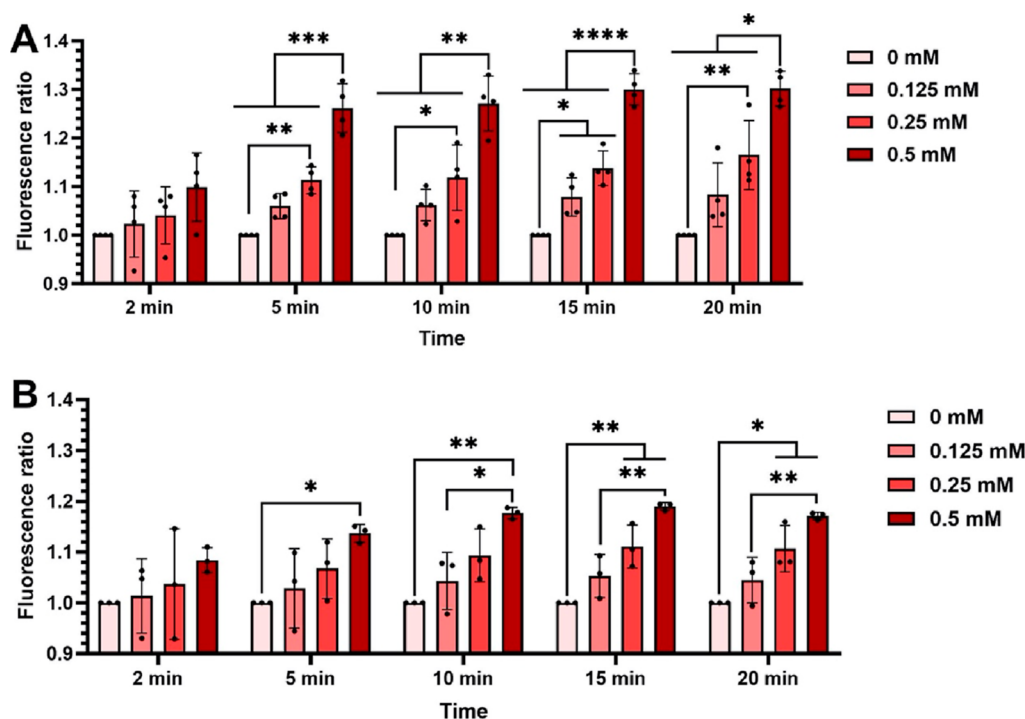


Figure 5. Ammonia sensing in ammonia-spiked mouse blood using a portable fluorometer. Fluorescence intensity ratio of IRDye 680RD-containing PS-*b*-PEG polymersomes in ammonia-spiked isotonic phosphate buffer of 50 mM at pH 7.4 over time (A). Fluorescence intensity ratio of IRDye 680RD-containing PS-*b*-PEG polymersomes in ammonia-spiked blood over time (B). Fluorescence intensity ratio: fluorescence intensity in ammonia-spiked buffer or blood normalized to nonspiked buffer or blood. Inner phase composition: dye concentration: 37 μ M; buffer composition of inner phase: isotonic citric acid buffer 2.5 mM at pH 2.0; whole blood volume fraction (B): 3% (v/v); incubation at room temperature. Detector: portable fluorometer. All results as means \pm SD ($n = 4$). ** $p < 0.01$, *** $p < 0.001$.

aggregation was observed (Figure S5). To study the selectivity of the assay for ammonia, polymersomes were incubated with ammonia and physiologically amine-containing metabolites and drugs (Figure S6). The absence or small increases in fluorescence intensity upon addition of these potentially interfering substances highlights the high selectivity of the assay to ammonia and is in accordance with the literature.⁹ Furthermore, the fluorescence intensity of the polymersomes was tested over the time of the assay in the absence of ammonia (Figure S7), and the stable fluorescence indicated that the transmembrane pH gradient of the polymersomes was stable during the assay.

3.3. Blood Ammonia Sensing Using a Portable Fluorometer

After the polymersome ammonia assay was tested using a conventional tabletop plate reader, its performance was tested using the portable fluorometer (Figure 1C). There was an ammonia concentration-dependent increase in fluorescence intensity in ammonia-spiked buffer (Figure 5A) and blood (Figure 5B). This finding demonstrates the usefulness of the portable fluorometer as a detector for the polymersome blood ammonia assay. The lower limit of quantification was 125 μ M after 2 min (coefficient of variation of 7.2%). The increase in fluorescence intensity ratio was lower, and the lower limit of quantification was higher than with the plate reader. This may be explained by the different excitation and emission wavelengths used by the plate reader and portable fluorometer. While we were able to use optimized wavelengths with the plate reader, thanks to its monochromator, the wavelengths could not be adjusted with the portable fluorometer.

4. CONCLUSIONS

Ammonia is a key biomarker in inborn and acquired liver disease, but point-of-care blood ammonia diagnostics are currently lacking. Here, we developed a polymersome formulation for blood ammonia sensing and combined it with a portable fluorometer. Building on an ammonia-selective PS-*b*-PEG polymersome technology, these polymersomes were loaded with a pH-sensitive NIR dye to minimize interference by hemoglobin in whole blood. Rapid and linear ammonia sensing was observed in whole blood in a clinically relevant range by using a conventional tabletop fluorometer. To translate the assay to clinics, it was tested with a portable fluorometer that requires small sample volumes and rapidly measures the fluorescence intensity. The motivation behind the use of a portable detection system is that it allows point-of-care (at home, doctor's office, pharmacy, and ambulance truck) and bedside (emergency room and intensive care unit) measurements. The portable fluorometer detected a pH-dependent fluorescence increase in the pH-sensitive NIR dye. The polymersome assay in combination with the portable reader performed well in ammonia-spiked buffer and whole blood. These findings highlight the blood ammonia sensing properties of the NIR dye-loaded PS-*b*-PEG polymersomes and strongly support the usefulness of the portable fluorometer as a detector, and they motivate a further clinical translation of this NIR fluorescent polymersome ammonia assay.

■ ASSOCIATED CONTENT

Data Availability Statement

The data sets generated during and/or analyzed during the current study are available from the corresponding author on reasonable request.

SI Supporting Information

The Supporting Information is available free of charge at <https://pubs.acs.org/doi/10.1021/acsbioimedchemau.4c00013>.

Structure of the IRDye680 RD, stability study of the dye in acidic buffer, depiction of Figure 4A as a histogram, intra- and interday variability study of the ammonia assay, stability study of the polymersomes, and selectivity study of the ammonia-sensing polymersomes (PDF)

■ AUTHOR INFORMATION

Corresponding Author

Simon Matoori – *Faculté de Pharmacie, Université de Montréal, Montreal, Quebec H3T 1J4, Canada*;
orcid.org/0000-0002-1559-0950; Phone: +1 514 343 6055; Email: simon.matoori@umontreal.ca

Authors

Marie-Lynn Al-Hawat – *Faculté de Pharmacie, Université de Montréal, Montreal, Quebec H3T 1J4, Canada*
Justine Caron – *Faculté de Pharmacie, Université de Montréal, Montreal, Quebec H3T 1J4, Canada*
Sarah Djebbar – *Faculté de Pharmacie, Université de Montréal, Montreal, Quebec H3T 1J4, Canada*

Complete contact information is available at:
<https://pubs.acs.org/doi/10.1021/acsbioimedchemau.4c00013>

Author Contributions

SM conceived and designed the study. Material preparation, data collection, and analysis were performed by MLAH, JC, and SD. The first draft of the manuscript was written by SM, and all authors commented on previous versions of the manuscript. All authors read and approved the final manuscript. CRediT: **Marie-Lynn Al-Hawat** data curation, investigation, visualization, writing-review & editing; **Justine Caron** data curation, investigation, visualization, writing-review & editing; **Sarah Djebbar** investigation, writing-review & editing; **Simon Matoori** conceptualization, funding acquisition, methodology, project administration, supervision, validation, writing-original draft, writing-review & editing.

Funding

S.M. gratefully acknowledges funding from the Natural Sciences and Engineering Research Council of Canada (Discovery Grant RGPIN-2022-04384), Canada Foundation for Innovation (Fonds des leaders John-R.-Evans 42712), and Fonds de recherche du Québec—Nature et technologies (Relève professorale 330153). M.L.A.H. gratefully acknowledges funding from the Faculty of Pharmacy at Université de Montréal (bourse du centenaire). S.D. gratefully acknowledges a summer scholarship from the Faculty of Pharmacy at Université de Montréal.

Notes

The authors declare the following competing financial interest(s): SM is a co-inventor on a patent application related to the technology described in this study.

Ethics approval: This study did not include in vivo experiments or experiments with human subjects.

Consent to participate: This study did not include experiments with human subjects.

■ ACKNOWLEDGMENTS

We thank Liliane Ménard (Université de Montréal) for providing the mouse blood.

■ REFERENCES

- (1) Matoori, S.; Leroux, J.-C. Recent advances in the treatment of hyperammonemia. *Adv. Drug Delivery Rev.* **2015**, *90*, 55–68.
- (2) Kroupina, K.; Bémeur, C.; Rose, C. F. Amino acids, ammonia, and hepatic encephalopathy. *Anal. Biochem.* **2022**, *649*, 114696.
- (3) Ott, P.; Vilstrup, H. Cerebral effects of ammonia in liver disease: current hypotheses. *Metab. Brain Dis.* **2014**, *29*, 901–911.
- (4) Jones, B. I.; Jenkins, C. A.; Murphy, D.; Orr, J.; Yeoman, A.; Hubbuck, E. R.; Heywood, B. R.; Currie, C. J. Predicting hepatic encephalopathy in patients with cirrhosis: A UK population-based study and validation of risk scores. *Hepatol. Commun.* **2023**, *7*, No. e0307.
- (5) Vilstrup, H.; Amodio, P.; Bajaj, J.; Cordoba, J.; Ferenci, P.; Mullen, K. D.; Weissenborn, K.; Wong, P. Hepatic encephalopathy in chronic liver disease: 2014 Practice Guideline by the American Association for the Study of Liver Diseases and the European Association for the Study of the Liver. *Hepatology* **2014**, *60*, 715–735.
- (6) Häberle, J.; Boddaert, N.; Burlina, A.; Chakrapani, A.; Dixon, M.; Huemer, M.; Karall, D.; Martinelli, D.; Crespo, P.; Santer, R.; et al. Suggested guidelines for the diagnosis and management of urea cycle disorders. *Orphanet J. Rare Dis.* **2012**, *7*, 32.
- (7) Ong, J. P.; Aggarwal, A.; Krieger, D.; Easley, K. A.; Karafa, M. T.; Van Lente, F.; Arroliga, A. C.; Mullen, K. D. Correlation between ammonia levels and the severity of hepatic encephalopathy. *Am. J. Med.* **2003**, *114*, 188–193.
- (8) Goldstein, B. N.; Wesler, J.; Nowacki, A. S.; Reineks, E.; Natowicz, M. R. Investigations of blood ammonia analysis: Test matrices, storage, and stability. *Clin. Biochem.* **2017**, *50*, S37–S39.
- (9) Matoori, S.; Bao, Y.; Schmidt, A.; Fischer, E. J.; Ochoa-Sanchez, R.; Tremblay, M.; Oliveira, M. M.; Rose, C. F.; Leroux, J. An investigation of PS-b-PEO polymersomes for the oral treatment and diagnosis of hyperammonemia. *Small* **2019**, *15*, No. e1902347.
- (10) Spyrogianni, A.; Gourmel, C.; Hofmann, L.; Marbach, J.; Leroux, J. C. Optimization of an ammonia assay based on transmembrane pH-gradient polymersomes. *Sci. Rep.* **2021**, *11*, 22032–22115.
- (11) Schmidt, A. C.; Hebels, E. R.; Weitzel, C.; Kletzmayer, A.; Bao, Y.; Steuer, C.; Leroux, J. Engineered Polymersomes for the Treatment of Fish Odor Syndrome: A First Randomized Double Blind Olfactory Study. *Adv. Sci.* **2020**, *7*, 1903697.
- (12) Giacalone, G.; Matoori, S.; Agostoni, V.; Forster, V.; Kabbaj, M.; Eggenschwiler, S.; Lussi, M.; De Gottardi, A.; Zamboni, N.; Leroux, J. C. Liposome-supported peritoneal dialysis in the treatment of severe hyperammonemia: An investigation on potential interactions. *J. Controlled Release* **2018**, *278*, 57–65.
- (13) Matoori, S.; Forster, V.; Agostoni, V.; Bettschart-Wolfensberger, R.; Bektas, R. N.; Thöny, B.; Häberle, J.; Leroux, J. C.; Kabbaj, M. Preclinical evaluation of liposome-supported peritoneal dialysis for the treatment of hyperammonemic crises. *J. Controlled Release* **2020**, *328*, 503–513.
- (14) Matoori, S.; Leroux, J.-C. Twenty-five years of polymersomes: lost in translation? *Mater. Horiz.* **2020**, *7*, 1297–1309.

- (15) Guirguis, N.; Bertrand, A. X.; Rose, C. F.; Matoori, S. 175 Years of Bilirubin Testing: Ready for Point-of-Care? *Adv. Healthcare Mater.* **2023**, *12*, 2203380.
- (16) Matoori, S.; Mooney, D. J. Near-Infrared Fluorescence Hydrogen Peroxide Assay for Versatile Metabolite Biosensing in Whole Blood. *Small* **2020**, *16*, 2000369.
- (17) Matoori, S.; Mooney, D. J. Development of a liposomal near-infrared fluorescence lactate assay for human blood. *Biomaterials* **2022**, *283*, 121475.
- (18) Babity, S.; Roohnikan, M.; Brambilla, D.; Babity, S.; Roohnikan, M.; Brambilla, D. Advances in the Design of Transdermal Micro-needles for Diagnostic and Monitoring Applications. *Small* **2018**, *14*, 1803186.
- (19) Babity, S.; Couture, F.; Campos, E. V. R.; Hedtrich, S.; Hagen, R.; Fehr, D.; Bonmarin, M.; Brambilla, D. A Naked Eye-Invisible Ratiometric Fluorescent Microneedle Tattoo for Real-Time Monitoring of Inflammatory Skin Conditions. *Adv. Healthcare Mater.* **2022**, *11*, 2102070.
- (20) Al-Hawat, M.-L.; Cherifi, K.; Tricou, L.-P.; Lamontagne, S.; Tran, M.; Ngu, A. C. Y.; Manrique, G.; Guirguis, N.; Machuca-Parra, A. I.; Matoori, S. Fluorescent pH-sensing bandage for point-of-care wound diagnostics. *Aggregate* **2023**, *5*, No. e472.
- (21) Fu, T.; Stupnitskaia, P.; Matoori, S. Next-Generation Diagnostic Wound Dressings for Diabetic Wounds. *ACS Meas. Sci. Au* **2022**, *2*, 377–384.
- (22) Mielczarek, W. S.; Obaje, E. A.; Bachmann, T. T.; Kersaudy-Kerhoas, M. Microfluidic blood plasma separation for medical diagnostics: is it worth it? *Lab Chip* **2016**, *16*, 3441–3448.
- (23) Guirguis, N.; Machuca-Parra, A. I.; Matoori, S. Portable Near-Infrared Fluorometer for a Liposomal Blood Lactate Assay. *ACS Pharmacol. Transl. Sci.* **2023**, *6*, 907–912.
- (24) Polomska, A. K.; Proulx, S. T.; Brambilla, D.; Fehr, D.; Bonmarin, M.; Brändli, S.; Meboldt, M.; Steuer, C.; Vasileva, T.; Reinke, N.; et al. Minimally invasive method for the point-of-care quantification of lymphatic vessel function. *JCI Insight* **2019**, *4*, 126515.
- (25) Nemiroski, A.; Ryou, M.; Thompson, C. C.; Westervelt, R. M. Swallowable fluorometric capsule for wireless triage of gastrointestinal bleeding. *Lab Chip* **2015**, *15*, 4479–4487.
- (26) Dukic, L.; Simundic, A.-M. Short-term and long-term storage stability of heparin plasma ammonia. *J. Clin. Pathol.* **2015**, *68*, 288–291.
- (27) Matoori, S.; Voznyuk Wuerthinger, O.; Leroux, J. Method of making a polymersome. U.S. Patent 20,230,220,165 A1, 2017.
- (28) Chow, S. L.; Gandhi, V.; Krywawych, S.; Clayton, P. T.; Leonard, J. V.; Morris, A. A. M. The significance of a high plasma ammonia value. *Arch. Dis. Child.* **2004**, *89*, 585–586.
- (29) Posset, R.; Garcia-Cazorla, A.; Valayannopoulos, V.; Teles, E. L.; Dionisi-Vici, C.; Brassier, A.; Burlina, A. B.; Burgard, P.; Cortès-Saladelafont, E.; Dobbelaere, D.; et al. Age at disease onset and peak ammonium level rather than interventional variables predict the neurological outcome in urea cycle disorders. *J. Inherited Metab. Dis.* **2016**, *39*, 661–672.
- (30) Bachmann, C. Outcome and survival of 88 patients with urea cycle disorders: a retrospective evaluation. *Eur. J. Pediatr.* **2003**, *162*, 410–416.
- (31) Grady, M.; Pineau, M.; Pynes, M. K.; Katz, L. B.; Ginsberg, B. A clinical evaluation of routine blood sampling practices in patients with diabetes: impact on fingerstick blood volume and pain. *J. Diabetes Sci. Technol.* **2014**, *8*, 691–698.